HHS Public Access

Author manuscript

Eur J Neurosci. Author manuscript; available in PMC 2021 February 01.

Published in final edited form as:

Eur J Neurosci. 2020 February ; 51(3): 866–880. doi:10.1111/ejn.14536.

The ventrolateral periaqueductal gray updates fear via positive prediction error

Rachel A. Walker[1], **Kristina M. Wright**[1], **Thomas C. Jhou**[2], **Michael A. McDannald**[1]

[1]Department of Psychology, Boston College, Chestnut Hill, MA

[2]Department of Neuroscience, Medical University of South Carolina, Charleston, SC

Abstract

Aversive, positive prediction error (+PE) provides a mechanism to update and increase future fear to uncertain threat predictors. The ventrolateral periaqueductal grey (vlPAG) has been offered as a neural locus for +PE computation. Yet a causal demonstration of vlPAG +PE activity to update fear remains elusive. We devised a fear discrimination procedure in which a danger cue predicts shock deterministically and an uncertainty cue predicts shock probabilistically, requiring prediction errors to achieve an appropriate fear response. Recording vlPAG single-unit activity during fear discrimination in Long-Evans rats, we reveal activity related to shock is consistent with +PE and updates subsequent fear to uncertainty at the trial level. We further demonstrate that vlPAG inhibition during shock selectively decreases future fear to uncertainty, but not danger, and temporal emergence of this effect is consistent with single-unit activity. These findings provide causal evidence that vlPAG +PE is necessary for fear updating.

Graphical Abstract

Materials & Correspondence: Please address correspondence and requests for material to R.A.W. (zacharir@bc.edu) or M.A.M. (michael.mcdannald@bc.edu).

Author contributions: K.M.W. performed the single-unit recording and electrode placement verification. T.C.J. designed and made the shock floor grounding device. R.A.W. performed the optogenetic testing and viral transfection and implant verification. R.A.W. and M.A.M. performed data analyses. The manuscript was written by R.A.W. and M.A.M and revised by all authors.

Competing Interests: The authors declare no competing interests.

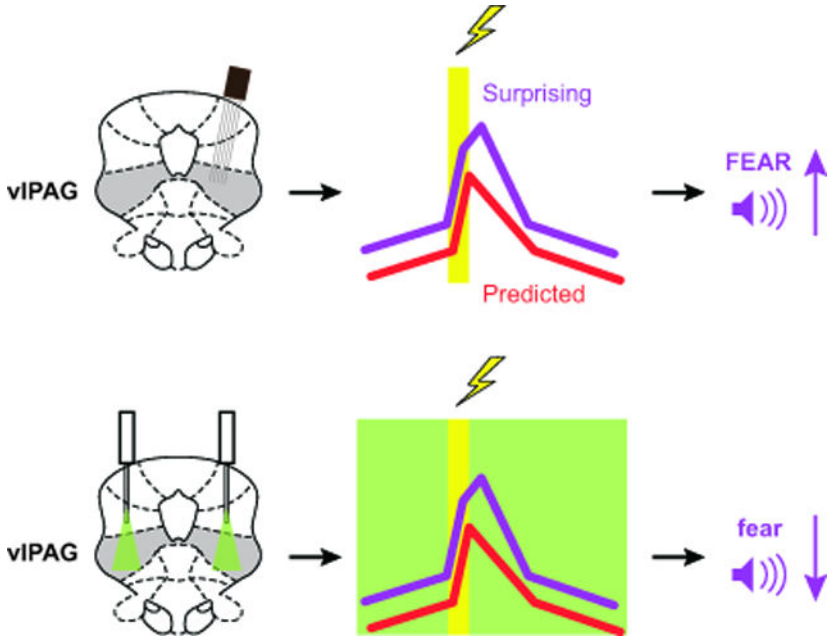

Single-unit activity in the ventrolateral periaqueductal grey (vlPAG) reflects positive aversive prediction error (+PE) and updates subsequent fear to uncertain threat predictors at the trial level in fear conditioning. Optogenetic inhibition of vlPAG activity around foot shock selectively decreases future fear to uncertain threat predictors and temporal emergence of this effect is consistent with single-unit activity. These findings casually implicate vlPAG +PE as necessary for fear updating.

Keywords

fear conditioning; conditioned suppression; sex; single-unit recording; optogenetics

Prediction errors – discrepancies between predicted and received outcomes – are learning signals that update cue-outcome associations to alter future behavior. Signed prediction errors come in two varieties: negative and positive. In aversive settings, negative prediction error occurs when the actual outcome is better than predicted (e.g. expecting a foot shock, but receiving none), weakening the cue-outcome association (Rescorla, 1970). Here we focus on positive prediction error (+PE), which occurs when an actual outcome is worse than predicted (e.g. not expecting a foot shock, but receiving one). Critically, +PE occurs at the time of foot shock, but updates and strengthens the cue-shock association (Rescorla & Wagner, 1972).

Neural activity consistent with +PE has been observed in the ventrolateral periaqueductal grey (vlPAG) (Johansen, Tarpley, LeDoux, & Blair, 2010; Roy et al., 2014), and modulating vlPAG activity alters predictive learning driven by +PE (Assareh, Bagley, Carrive, & McNally, 2017; Cole & McNally, 2009; McNally & Cole, 2006; Ozawa et al., 2017). VlPAG/dorsal raphe dopamine/glutamate neurons regulate nociceptive behavior (Li et al., 2016) and have been offered as a possible source of the +PE (Groessl et al., 2018). However,

this population is responsive to a wide variety of 'salient' biologically significant events such as foot shock, conspecifics, and reward (Cho et al., 2017). Biological salience is here operationally defined as in Cho and colleagues (2017), referring to stimuli producing an unconditioned response. Still, lacking in the current literature is evidence that vlPAG +PE activity updates within-session fear to a predictive cue. This is despite the fact that such updating would be an expected consequence of strengthening the cue-shock association.

In two experiments, we sought to uncover a relationship between vlPAG +PE activity and fear updating. We employed a fear discrimination procedure in which a danger cue predicted shock deterministically, and an uncertainty cue predicted shock probabilistically (Berg, Schoenbaum, & McDannald, 2014; Walker, Andreansky, Ray, & McDannald, 2018; Wright, DiLeo, & McDannald, 2015). In experiment 1, we recorded vlPAG single-units during ongoing fear discrimination, focusing on activity around predicted (danger) and surprising (uncertainty) foot shock delivery. Analyses examined the relationship between neural activity following foot shock and fear updating. In experiment 2, we selectively inhibited vlPAG activity around the time of predicted and surprising foot shock delivery. Analyses focused on subsequent changes in fear to the danger and uncertainty cues and the temporal emergence of these changes. Combined, the experiments allowed us to determine if a +PE signal is observed in vlPAG neurons and if this signal is necessary to update and increase future fear.

Results

We devised a within-subjects fear discrimination procedure to distinguish vlPAG signaling of biological salience from +PE, and to explicitly examine the relationship between vlPAG activity and fear updating (Fig. 1A). In the procedure, three auditory cues predict unique foot shock probabilities: danger ($p = 1.00$), uncertainty ($p = 0.375$), and safety ($p = 0.00$). Using conditioned suppression of rewarded nose poking as our dependent measure, we have previously found excellent discriminative fear in male and female rats: high to danger, intermediate to uncertainty, and low to safety (Berg et al., 2014; DiLeo, Wright, & McDannald, 2016; Ray, Hanlon, & McDannald, 2018; Walker et al., 2018; Wright et al., 2015). Theoretically, +PEs provide an updating mechanism that would permit fear to uncertainty to remain at an intermediate level. Practically, +PEs would be perpetually generated to shock receipt on uncertainty trials because the random order of shock and omission trials keeps receipt 'surprising.' By contrast, shock receipt on danger trials would be 'predicted,' and +PEs should be virtually absent. Importantly, foot shock events are identical for uncertainty and danger, meaning differential firing on uncertainty and danger trials must reflect predictiveness rather than biological salience.

Shock-responsive vlPAG firing is an amalgam of biological salience and +PE

We recorded 245 single-units from 6 male Long Evans rats over 88 sessions of fear discrimination (electrode placements shown in Fig. 1B). We identified 26 neurons from 5 subjects (subject 1: 8 neurons, subject 2: 5 neurons, subject 3: 3 neurons, subject 4: 9 neurons and subject 5: 1 neuron) showing phasic increases in firing over baseline around shock periods on uncertainty *or* danger trials (two-tailed, paired samples t-test, $p < 0.025$;

Bonferroni correction for two tests). During the 26 sessions in which shock-responsive neurons were identified, rats showed excellent fear discrimination (Fig. 1C). ANOVA for suppression ratio revealed a main effect of cue ($F_{3,75} = 132.4$, $p = 6.98 \times 10^{-30}$, $\eta_p^2 = 0.84$, op = 1.00), and post-hoc t-tests confirmed that suppression ratios differed for every trial-type comparison [all $t > 8$, all $p < 1.01 \times 10^{-8}$, except for uncertainty-omission vs. uncertainty-shock ($t = 1.38$, $p = 0.18$), which were not expected to differ]. Critically, rats consistently showed intermediate fear to uncertainty. Firing from a representative shock-responsive neuron is shown in Figure 1D.

Plotting shock-responsive population activity (Fig. 1E) reveals an amalgam of biological salience and +PE. Pre-shock firing to danger and uncertainty gives way to non-selective increases during foot shock (biological salience), followed by selectively enhanced firing on uncertainty trials (+PE). In support, ANOVA for z-score normalized firing rates [factors: interval (100-ms, 50 bins, 5 s following cue offset) and trial type (danger, uncertainty-shock, uncertainty-omission, and safety)] revealed a main effect of trial type ($F_{3,75} = 35.14$, $p = 2.72 \times 10^{-14}$, ηp^2; = 0.58, op = 1.00) and a trial type x interval interaction ($F_{147,3675} = 3.60$, $p = 1.26 \times 10^{-40}$, $\eta p^2 = 0.13$, op = 1.00). Maximal differential firing occurred immediately following foot shock (Fig. 1E). ANOVA for normalized firing during this 500-ms interval revealed a main effect of trial type ($F_{3,75} = 39.84$, $p = 1.66 \times 10^{-15}$, $\eta p^2 = 0.61$, op = 1.00), and post-hoc t-tests found significant differential firing for all comparisons (danger vs uncertainty-shock, $t = 4.06$, $p = 0.00004$; danger vs uncertainty-omission, $t = 3.35$, $p = 0.003$; uncertainty-omission vs safety, $t = 3.88$, $p = 0.001$). Corroborating the population analysis, single-unit firing in the 500-ms post-shock period was correlated on danger and uncertainty-shock trials (Fig. 1F; $R^2 = 0.36$, $p = 0.0012$), but single-units were biased toward greater firing on uncertainty-shock trials (sign test = 0.043). Plotting differential firing by subject revealed relatively uniform, positive values across subjects (Fig. 3G), with the exception of subject 5 from whom only one shock-responsive neuron was recorded.

Shock-responsive vlPAG neurons signal +PE

Descriptive firing analyses reveal signals for biological salience as well as +PE. So how can we disentangle these two theoretical signals? If vlPAG neurons primarily signal biological salience, then signaling of predicted shock (danger trials) and surprising shock (uncertainty trials) should show synchronous temporal patterns. By contrast, if vlPAG neurons primarily signal +PE, predicted shock signaling should be observed *prior* to shock delivery, while surprising shock signaling should transiently dominate *following* shock delivery.

To formally test signaling of surprising versus predicted foot shock, we used simultaneous linear regression for single-unit firing. For each shock-responsive vlPAG single-unit, we calculated the normalized firing rate for each trial type (32 total: 6 danger, 6 uncertainty shock, 10 uncertainty omission, and 10 safety) in 500 ms intervals over the 5 s post-cue period. The ‘predicted’ regressor assigned the following values to each trial type: (danger = 2, unc-shock = 1, unc-omission = 0, safety = 0), while the ‘surprising’ regressor assigned: (danger = 1, unc-shock = 2, unc-omission = 0, safety = 0). Output for each single-unit was a beta coefficient for each regressor, quantifying the strength (|>0| = stronger) and direction (>0 = positive) of the predictive relationship between firing and each regressor in each

interval. Beta coefficients were subjected to ANOVA with regressor (predicted vs. surprising) and interval (500 ms intervals for 5 s post-cue period) as factors. Single-unit regression allowed us to determine the relative contribution of each regressor to each single-unit over the post-cue period. ANOVA revealed a main effect of interval ($F_{9,225} = 7.57$, $p = 1.22 \times 10^{-9}$, $\eta p^2 = 0.23$, op = 1.00) and interval x regressor interaction ($F_{9,225} = 3.06$, $p = 0.002$, $\eta p^2 = 0.11$, op = 0.97) (Fig. 1H). Positive beta coefficients for the predicted regressor were observed prior to shock then diminished. This was due to residual cue signaling by shock-responsive neurons (Fig. S1A). Consistent with +PE signaling, positive beta coefficients for the surprising shock regressor were only observed during and immediately following shock delivery. Beta coefficients in the 500 ms immediately following foot shock significantly differed for predicted vs. surprising regressors (Fig. 1I; two-tailed t-test, $t_{25} = 4.06$, $p = 0.0004$). The temporal patterns for predicted (pre shock > post shock) and surprising shock signaling (post shock > pre shock) were observed across shock-responsive vlPAG single-units but were unrelated (Fig. 1J). These temporal firing patterns were observed in each subject (Fig. 1K) and are consistent with +PE activity in the vlPAG.

vlPAG inhibition during foot shock selectively reduces subsequent fear to uncertainty

Single-unit recording reveals a neural correlate for +PE in shock-responsive vlPAG neurons but does not demonstrate a causal role for shock-related activity to selectively modulate fear to uncertainty. If shock-responsive vlPAG neurons signal +PE, then inhibition of neural activity at the time of surprising foot shock should reduce fear to uncertainty, but inhibition during predicted foot shock would have no effect on fear to danger. By contrast, if the vlPAG activity reflects biological salience, then inhibiting foot shock activity should non-selectively reduce fear to uncertainty and danger.

Rats received bilateral vlPAG transfection with halorhodopsin (eNpHR, AAV5-hSyn-eNpHR3.0-EYFP; n = 6; 3 females) or a control fluorophore (YFP, AAV5-hSyn-EYFP; n = 7; 4 females) and bilateral implantation of optical ferrules over the vlPAG (Fig. 2A, B). Rats were trained on a modified version of the fear discrimination procedure (sessions: 16 untethered, 3 tethered, 3 light illumination and 3 untethered) utilizing the same foot shock probabilities but presenting fewer trials per session (18 total: 6 danger, 3 uncertainty shock, 5 uncertainty omission, and 4 safety). This was done to make discrimination proceed more slowly, maintaining higher fear to uncertainty longer. The optogenetic manipulation (Fig. 2C) was hypothesized to decrease fear to the uncertainty cue, so higher fear to uncertainty was needed to ensure detection of decreased fear. All rats showed bilateral transfection in the lateral and ventrolateral PAG with ferrules tips just inside the vlPAG boundary (Fig. 2A, B). Expression was relatively uniform across individuals and there were no relationships observed between transfection area and fear behavior. YFP and eNpHR rats did not differ in baseline nose poke behavior, which was supported by ANOVA demonstrating no main effect of, or interaction with, group during discrimination (Fig. S2A; all $F < 1.3$, all $p > 0.28$) or the optogenetic manipulation (Fig. S2B; all $F < 1.40$, all $p > 0.27$). However, a significant effect of sex was found during discrimination ($F_{1,9} = 6.20$, $p = 0.034$), with males poking at higher rates than females. A similar trend toward significance was found during the optogenetic manipulation ($F_{1,9} = 4.88$, $p = 0.055$).

YFP (Fig. 2C) and eNpHR (Fig. 2D) rats acquired high fear to danger and uncertainty but low fear to safety over discrimination. Females demonstrated overall higher fear compared to males (main effect of sex $F_{1,9} = 8.34$, $p < 0.05$, $\eta^2_p = 0.48$, power = 0.73), and YFP rats demonstrated overall higher fear compared to eNpHR rats (YFP group had higher proportion of females). Importantly, eNpHR and YFP rats showed equivalent discrimination (Fig. 2D, E). These findings were supported by a main effect of group ($F_{1,9} = 6.31$, $p < 0.05$, $\eta^2_p = 0.41$, power = 0.61), cue ($F_{2,18} = 30.87$, $p < 0.001$, $\eta^2_p = 0.77$, power = 1.00), session ($F_{18,162} = 12.95$, $p < 0.001$, $\eta^2_p = 0.59$, power = 1.00), and a cue x session interaction ($F_{36,324} = 6.20$, $p < 0.001$, $\eta^2_p = 0.41$, power = 1.00). There were no interactions between group and cue (all $F < 2.15$, $p > 0.05$). Differences in trial number account for inequality of absolute fear levels during discrimination between rats used for single-unit recordings versus optogenetics (see Fig. 1C, 2D–E). Thus, at the start of the optogenetic manipulation, eNpHR and YFP rats showed equivalent fear discrimination.

Over the three illumination sessions, green light (532 nm, 25 mW) was delivered for the 4-second period following cue offset on danger and uncertainty-shock trials (2-second delay, 0.5-second shock and 1.5-second post shock; Fig. 2C). Illumination parameters were identical for YFP and eNpHR groups, but only in the eNpHR group would vlPAG activity be inhibited. Notably, no illumination occurred during the 10-s cue period, during which fear was measured. While YFP and eNpHR rats showed equivalent levels of fear to all cues in the first illumination session, discrimination diverged thereafter (Fig. 2F). ENpHR rats markedly reduced fear to uncertainty, but not danger; YFP rats showed no changes in fear to either cue. This pattern continued through the 3 no-illumination untethered sessions, and results were confirmed by ANOVA, which found a cue x session x group interaction ($F_{10,90} = 2.59$, p = 0.0084, $\eta^2_p = 0.22$, power = 0.94). This interaction was driven by decreased fear to uncertainty in eNpHR rats (Fig. 2G). This pattern was apparent in both sexes, with subtle sex effects and interactions observed for uncertainty and safety (Fig. S3). These results are inconsistent with a role for vlPAG shock activity in biological salience, which would have predicted reduced fear to danger and uncertainty, but support a specific and causal role for vlPAG in +PE.

Finally, while ANOVA found no cue x group interaction for pre-opto discrimination, it visually appeared as though eNpHR rats achieved better discrimination. It is then possible that the low uncertainty fear observed prior to illumination sessions was explained by low uncertainty fear at the end of discrimination. To examine this possibility, we plotted individual fear to uncertainty during the final three discrimination sessions (mean) versus fear to uncertainty during the three post-illumination sessions (Fig. 2H). Consistent with no effect of light illumination on YFP individuals, there was a positive correlation between fear to uncertainty at the end of discrimination and following illumination ($R^2 = 0.75$, p = 0.012). In eNpHR individuals, there was no relationship ($R^2 = 0.047$, p = 0.68). All eNpHR individuals showed low fear to uncertainty following light illumination regardless of the level shown in discrimination. Light illumination thus actively reduced fear to uncertainty only in eNpHR rats.

Single-unit trial +PE activity predicts fear updating to uncertainty

Shock-responsive vlPAG neurons show neural activity patterns consistent with +PE signaling and optogenetic inhibition of vlPAG shock activity selectively reduces fear to uncertainty, consistent with a causal role in +PE. However, these findings do not explicitly link vlPAG +PE to fear updating. To test this link, we examined the relationship between single-trial shock activity and trial-by-trial changes in fear to uncertainty for the 26 shock-responsive vlPAG units. For each single-unit we selected the first three uncertainty-shock trials (n) in the session then identified the next three uncertainty trials (n+1, n+2 and n+3) regardless of shock delivery or omission. This produced a total of 78 (26 × 3) trial sequences. Differential firing on each trial 'n' was calculated by taking normalized firing to uncertainty-shock in the 500-ms post-shock period and subtracting mean normalized firing to all danger trials in the same time period. Positive values would indicate greater firing to surprising shock over predicted shock, consistent with +PE. Uncertainty suppression ratios were calculated for each trial as previously described.

Of the 78 trial sequences, 7 showed differential firing or changes in suppression ratios $|>2|$ standard deviations from the group mean. These 7 outliers were removed and analysis of covariance (ANCOVA) for suppression ratios in the remaining 71 sequences revealed that differential firing on trial 'n' (covariate) informed trial-by-trial changes in suppression ratio to uncertainty (trial: n, n+1, n+2, n+3). This was substantiated by a significant differential firing x trial interaction ($F_{1,69} = 5.21$, $p = 0.026$, $\eta p^2 = 0.07$, op = 0.62). Positive differential firing on trial 'n' predicted increases in fear over the next 3 uncertainty trials while negative differential firing predicted decreases in fear (Fig. 3A, B). This relationship was observed across the 71 sequences, with greater differential firing predicting greater increases in fear to uncertainty (Fig. 3C), consistent with +PE fear updating.

vlPAG inhibition during foot shock blocks fear updating to uncertainty

VlPAG +PE activity predicted fear updating to uncertainty but this took ~3 trials to fully emerge. Given that our optogenetic procedure utilized only 3 uncertainty-shock trials per session, this would explain why no change in fear was observed during the first illumination session. Instead, optogenetic inhibition would be expected to block +PE fear updating to uncertainty *within* the second illumination session. Further, if vlPAG activity is specific to prediction error updating, no such within-session change should be observed to danger.

We isolated the second illumination session and identified the first uncertainty shock trial (n), as well as the next three uncertainty trials (n+1, n+2 and n+3) regardless of shock delivery or omission, for each individual (YFP and eNpHR). The same was done for the four danger trials (n, n+1, n+2 and n+3). Suppression ratios were calculated for each cue/trial. ANOVA for suppression ratios [factors: trial (4), group (YFP vs eNpHR), cue (danger vs. uncertainty) and sex (female vs. male)] revealed a group x trial x cue interaction ($F_{3,27} = 3.32$, $p = 0.035$, $\eta p^2 = 0.27$, op = 0.69). This interaction was the result of eNpHR and YFP rats showing equivalent fear to uncertainty in the first two trials but eNpHR rats selectively reducing to uncertainty in the remaining two trials (Fig. 3D). Comparing the change in fear in these two groups produced a pattern like that observed for vlPAG activity (compare Fig.

3A & 3D, Fig. 3B & 3E). T-test for change in fear falls just short of significance (YFP vs eNpHR, $t_{11} = 2.14$, $p = 0.056$), indicating the optogenetic manipulation led to decreases in fear over trials. This pattern did not emerge for danger, with YFP and eNpHR rats showing equivalent fear levels throughout the session (Fig. F) and no change over the session (Fig. 3G). This temporal pattern echoes that of endogenous +PE updating found in vlPAG single-units.

Discussion

Here we have shown that vlPAG activity to foot shock is better captured by +PE, compared to biological salience, and trial-by-trial fluctuations in single-unit firing predict subsequent changes in fear to uncertainty. Further, we demonstrate that inhibition of vlPAG activity precisely at the time of +PE updates and reduces future fear in a manner that mirrors the neural response. These results are consistent with the theoretical framework of our behavioral task requiring the use of prediction errors; by preventing +PEs on uncertainty-shock trials but leaving intact negative prediction errors on uncertainty-omission trials, eNpHR rats should only effectively receive neural signals to decrease fear to uncertainty, which matches the resultant behavioral reduction in fear. Our findings complement and extend previous studies demonstrating +PE correlates in the vlPAG (Groessl et al., 2018; Johansen et al., 2010; Roy et al., 2014) and critical roles for the vlPAG in predictive learning (Cole & McNally, 2009; McNally & Cole, 2006). Our results are also consistent with a neural circuit framework positing that the critical comparison of expected and actual foot shock takes place in the vlPAG (McNally, Johansen, & Blair, 2011).

Before discussing the implications of these findings, some caveats should be noted. The recording experiment utilized only males, while optogenetic inhibition tested both males and females. So while it is possible, albeit unlikely, that vlPAG +PE correlates would not be found in females, vlPAG foot shock activity at the time of +PE is critical to fear updating in both sexes. Previous experiments related to aversive prediction error signaling using rodents have been conducted using only males (Assareh et al., 2017; Cole & McNally, 2009; Groessl et al., 2018; Johansen et al., 2010; McNally & Cole, 2006; Ozawa et al., 2017), and one study in humans used both males and females but did not consider sex as a factor in their analyses (Roy et al., 2014). Sex differences in baseline behavior (i.e. nose poke rate and absolute fear levels) in the optogenetics results are consistent with previous findings in the same behavioral task (Walker et al., 2018). While the effect of optogenetic inhibition to decrease fear to uncertainty was observed across sexes, subtle interactions with sex and the pattern of fear to uncertainty and safety were observed. Given the relatively low number of subjects used here, future experiments of aversive prediction error signaling should continue to consider biological sex as a factor.

Another interesting feature of the data concerns post-optogenetics fear behavior. Reduced fear to uncertainty emerged during optogenetic inhibition in eNpHR rats and continued in the following no-illumination sessions. On first impression this is quite odd, as +PE should be fully intact in the no-illumination sessions. However, recall that experiment 1 demonstrated that with sufficient experience, rats readily discriminate uncertainty ($p = 0.375$) from danger ($p = 1.00$). The most parsimonious explanation is that YFP and eNpHR

would have eventually achieved discrimination, and optogenetic inhibition served to facilitate reduction of fear to uncertainty in eNpHR rats by reducing +PE. Along the same lines, reducing trial numbers per session in the optogenetic inhibition experiment resulted in higher fear levels to uncertainty through discrimination. This was necessary in order to detect reduced fear to uncertainty during and following illumination sessions.

Concerning anatomy, recording and optogenetic inhibition primarily targeted vlPAG but also included portions of lateral PAG. Although our observed correlates and behavioral effects are more consistent with those reported in vlPAG (Assareh, Sarrami, Carrive, & McNally, 2016), we cannot entirely rule out some contribution of the lateral PAG. Finally, we did not observe a correlate for negative prediction error (increased firing to shock omission on uncertainty trials) and therefore did not target optogenetic inhibition to this period. Unlike ventral tegmental area dopamine neurons that can produce positively and negatively signed reward prediction errors (Roesch, Calu, & Schoenbaum, 2007; Schultz, Dayan, & Montague, 1997), vlPAG neurons only appear to produce a +PE. Of course, reward settings permit many more trials per sessions, allowing for greater observation of a variety of prediction errors signals within a single session (Calu, Roesch, Haney, Holland, & Schoenbaum, 2010; Roesch, Calu, Esber, & Schoenbaum, 2010). Interestingly, evidence exists for dorsal raphe contribution to negative prediction error (Berg et al., 2014), an adjacent brain region reciprocally connected to the vlPAG (Beitz, 1982).

The present results are particularly relevant to those from recent study by Assareh and colleagues (Assareh et al., 2017). In this study, the l/vlPAG was photo inhibited during acquisition of a new cue-shock association, specifically at the time of foot shock. They found that in a subsequent extinction test rats that had received foot shock photo inhibition showed *greater* fear to the conditioned cue. This would appear to directly oppose our present findings. Recall that prediction error is the discrepancy between predicted and received shock. Assareh and colleagues (2017) argue that inhibiting vlPAG during the time of foot shock effectively blocked the prediction signal. The result was a larger, positive discrepancy between the predicted and actual shock, producing a larger +PE and further strengthening the cue-shock association. In reality, our results are consistent with those of Assareh in colleagues (2017). We observe vlPAG signals for ‘prediction’ prior to shock delivery and critically, even during shock presentation. A vlPAG signal for ‘+PE’ – the discrepancy – is not maximal until the seconds following shock offset. Our optogenetic manipulation was designed to inhibit during this post-shock period, as well as the pre-shock period. Thus, inhibiting vlPAG activity only during the pre-shock or shock period would be expected to strengthen cue-shock associations, while inhibiting during the post-shock period would be expected to weaken cue-shock associations.

Computing error requires a comparison of predicted and actual outcomes. While shock-responsive vlPAG neurons are cue-responsive in a manner that resembles prediction, there was no relationship between +PE activity and predictive signaling (Fig. S1B, C). Signals for prediction are then very likely to arise from distal brain regions. The central amygdala may provide such an input (Ozawa et al., 2017), but additional brain regions are likely involved. In particular, the vlPAG receives dense prefrontal inputs, including those from dorsomedial prefrontal cortex (Rozeske et al., 2018), prelimibic cortex (Beitz, 1982), medial/ventral/

dorsolateral divisions of orbital cortex, and dorsal/posterior divisions of agranular insular cortex (Floyd, Price, Ferry, Keay, & Bandler, 2000). Each of these prefrontal regions play essential and unique roles in fear learning and/or expression (Ray et al., 2018; Rozeske et al., 2018; Sarlitto, Foilb, & Christianson, 2018; Vidal-Gonzalez, Vidal-Gonzalez, Rauch, & Quirk, 2006; Yau & McNally, 2015) and are likely to provide overlapping and distinct predictions about impending aversive outcomes to the vlPAG. Additionally, the vlPAG is anatomically well-positioned to receive information about actual shock outcomes, as it receives direct and indirect nociceptive inputs from the dorsal horn (Todd, 2010). The vlPAG is then positioned at an intersection of signals for predicted and actual shocks, a requirement for computing a prediction error. In light of this anatomy, the current results present a compelling case for vlPAG as the neural locus of +PE to causally strengthen cue-shock association and update fear.

Further questions remain within the vlPAG, namely, what neuron types compute +PE and to where is this signal broadcast. Tyrosine hydroxylase positive (TH+), a dopamine/norepinephrine neuron marker, vlPAG neurons are shock-responsive and show learning-related changes in firing consistent with +PE. These TH+ neurons also typically contain the vesicular glutamate transporter 2 (vGluT2), a glutamatergic marker (Li et al., 2016; Matthews et al., 2016). However, a separate TH+/VgluT2+ population is primarily cue onset-responsive (Groessl et al., 2018). This population also shows learning-related changes in firing, but is largely distinct from the shock population. Here we also report that shock-responsive vlPAG neurons are not strongly cue onset-responsive. These populations must then be separated by additional genetic markers or perhaps by their connectivity, for example, those with innervation by dorsal horn nociceptive inputs (shock-responsive) vs central auditory inputs (cue-responsive). The vlPAG/dorsal raphe region is highly heterogeneous, most notably containing serotonergic neurons that are strongly activated by foot shock (Grahn et al., 1999; Schweimer & Ungless, 2010). So while clues to the neuron type identity can be found, further work is necessary. As for the target(s) of the vlPAG +PE, the midline/intralaminar thalamus has been offered (McNally et al., 2011; Sengupta & McNally, 2014). The vlPAG projects to a host of brain regions implicated in prediction and prediction error, including the major dopamine containing regions (A8 retrorubral field, A9 substantia nigra and A10 ventral tegmental area) (Watabe-Uchida, Zhu, Ogawa, Vamanrao, & Uchida, 2012), the diagonal band, and the lateral bed nucleus of the stria terminalis (Beitz, 1982). The relevant question may not be which vlPAG projection carries +PE, but how does each vlPAG +PE projection affect aversive cue signaling in each target region.

Exaggerated fear responses are a hallmark of stress and anxiety disorders and may be due in part to aberrant processing of uncertain threats (Grupe & Nitschke, 2013). However, excessive threat processing is not limited to disorders of anxiety. Adults maltreated as children show exaggerated neural responses to threatening stimuli despite the lack of any clinical diagnosis (Dannlowski et al., 2012), and our laboratory has shown that early adolescent adversity inflates fear to uncertainty in rodents (Walker et al., 2018; Wright et al., 2015). While speculative, the current results offer a potential mechanism by which exaggerated +PE activity in vlPAG neurons could drive excessive fear to ambiguous, threatening cues. There are currently no experiments, however, linking dysregulated prediction error signaling to disordered fear behavior. Future studies examining vlPAG +PE

signaling may then provide insight into a more complete neural circuit for normal and aberrant threat processing.

Methods

CONTACT FOR REAGENT AND RESOURCE SHARING

Further information and requests for resources and reagents should be directed to and will be fulfilled by the Lead Contact, Michael A. McDannald (michael.mcdannald@bc.edu).

Method Details

Experimental subjects: For single-unit recordings, final subjects were 6 adult male Long-Evans rats weighing 241 – 268 g upon arrival on postnatal day 55 (Charles River Laboratories, Raleigh, NC). All rats were implanted with drivable microelectrode bundles (−7.80 AP, ±1.77 ML, −5.89 DV from skull at ±10° angle), and the experimental design was completely within-subjects, yielding a single group. Sixteen individual recording wires were bundled and soldered to individual channels of an Omnetics connector. The bundle was integrated into a microdrive permitting advancement in ~0.042 mm increments. The microdrive was cemented on top of the skull and the Omnetics connector was affixed to the head cap. Implants were secured to the skull using dental cement (Henry Schein) and surrounded by a 50 mL centrifuge tube cut to create an enclosure around the electrode implant to prevent possible damage. Post-surgery, rats received 11 days of undisturbed recovery with prophylactic antibiotic treatment (cephalexin; Henry Schein, Melville, NY) before beginning fear discrimination. Four rats were excluded from analyses, one due to incorrect electrode placement and three for a failure to yield single-units.

For optogenetic inhibition, final subjects were 7 female and 6 male adult Long-Evans rats (Charles River Laboratories, Raleigh, NC). All rats underwent stereotaxic surgery under isofluorane (Henry Schein) anesthesia. Rats received 0.3 μl bilateral infusions of halorhodopsin (AAV5-hSyn-eNpHR3.0-EYFP; n = 6; 3 females) or YFP (AAV5-hSyn-EYFP; n = 7; 4 females) in the vlPAG (−7.80 AP, ±1.77 ML, −5.89 DV from skull at ±10° angle). Ten minutes elapsed before the syringe was withdrawn to allow for viral diffusion. Fiber optic ferrules were bilaterally implanted just above the infusion sites (−5.69 DV from skull at ±10° angle) to permit 532 nm light illumination. Implants were secured with dental cement surrounded by a cut centrifuge tube similar to that for single-unit recording. Post-surgery, rats received 2 weeks of undisturbed recovery with prophylactic antibiotic treatment (cephalexin; Henry Schein) before beginning fear discrimination. In order to be considered for analysis, rats had to maintain a nose poke rate higher than 5 poke/min (low rates make suppression ratios unreliable) and had to show a suppression ratio to uncertainty above 0.25 (in order to have room to observe decreases in fear). Six rats were excluded from analyses, three based on nose poke criteria and three based on suppression ratio criteria.

All rats were maintained on a 12-hour light-dark cycle (lights on 0600 – 1800). Rats were single housed and food restricted to 85% of their free-feeding body weight during Pavlovian fear conditioning with standard laboratory chow (18% Protein Rodent Diet #2018, Harlan Teklad Global Diets, Madison, WI). Water was available *ad libitum* in the home cage but

was not available during behavioral testing, at which time only Dustless Precision Test Pellets (Bio-Serv: Cat #F0021) were present. All protocols were approved by the Boston College Animal Care and Use Committee, and all experiments were carried out in accordance with the NIH guidelines regarding the care and use of rats for experimental procedures.

Apparatus: The apparatus for Pavlovian fear discrimination consisted of six, individual sound-attenuated enclosures that each housed a behavior chamber with aluminum front and back walls, clear acrylic sides and top, and a metal grid floor. Each grid floor bar was electrically connected to an aversive shock generator (Med Associates, St. Albans, VT). A single food cup and a central nose poke opening, equipped with infrared photocells, were present on one wall. Auditory stimuli were presented through two speakers mounted on the ceiling of each sound-attenuated enclosure. Behavior chambers were modified to allow for free movement of the electrophysiology and optical cables during behavior; plastic funnels were epoxied to the top of the behavior chambers with the larger end facing down, and the tops of the chambers were cut to the opening of the funnel. Green (532 nm, 500 mW) lasers (Shanghai Laser & Optics Century Co., Ltd.; Shanghai, China) were used to illuminate the vlPAG. Optical cables were connected to the lasers via 1×2 fiber optic rotatory joints (Doric; Quebec, Canada). Rats were bilaterally connected to the optical cables by a ceramic sleeve placed over the implanted ferrule and ceramic ferrule end of the cable. Black shrink-wrap was also placed on the ends of the cables to block light emission into the behavioral chamber. A PM160 light meter (Thorlabs; Newton, NJ) was used to measure light output.

Nose poke acquisition: Before behavioral testing began, all rats were given 2 days of pre-exposure in the home cage to the pellets used for rewarded nose poking. Rats were then shaped to nose poke for these pellets in the experimental chamber. During the first session, rats were issued one pellet every 60 seconds with the nose poke port removed for 30 minutes. Rats were then issued pellets on a fixed ratio schedule in which one nose poke yielded one pellet until they reached at least 50 nose pokes (FR1) in a session. Over the next 5 days, rats were reinforced for nose pokes on a variable interval schedule first on average every 30 seconds (VI-30), for one session, then on average every 60 seconds (VI-60), for four sessions. All subsequent conditioning sessions were run with a background VI-60 reinforcement schedule that was completely independent of auditory cue or foot shock presentation on conditioning trials. For in vivo recordings, rats were trained through 8 days of fear discrimination before receiving surgery and returning to behavioral testing. For optogenetics, rats were trained through the four VI-60 sessions then underwent surgery and recovery before receiving two reminder VI-60 sessions and beginning pre-exposure.

Pre-exposure: In two separate sessions, each rat was pre-exposed to the three 10 s auditory cues to be used in Pavlovian fear discrimination. These 42 min sessions consisted of four presentations of each cue (12 total presentations) with a mean inter-trial interval (ITI) of 3.5 min. The order of trial type presentation was randomly determined by the behavioral program, and differed for each rat during each session. Auditory cues consisted of repeating motifs of: broadband click, phaser or trumpet and can be found here: http://

mcdannaldlab.org/resources/ardbark. Extensive testing has found these cues to be equally salient, yet discriminable.

Fear discrimination: For Experiment 1, each rat received eight, 93-minute sessions of fear discrimination prior to electrode implant. For the optogenetic inhibition, each rat received 16, 67-minute sessions of fear discrimination before the optogenetic manipulation. Auditory cues were 10 s in duration and consisted of repeating motifs of a broadband click, phaser, or trumpet. Every session began with a 5-minute habituation period, and ITIs were 3.5 minutes on average. Each cue was associated with a unique probability of foot shock (0.5 mA, 0.5 s): danger, p = 1.00; uncertainty, p = 0.375; and safety, p = 0.00. Foot shock was administered 2 s following the termination of the auditory cue on danger and uncertainty-shock trials. For the recording experiment, there were 32 trials per session consisting of 6 danger trials, 10 uncertainty no-shock trials, 6 uncertainty shock trials, and 10 safety trials. Animals received discrimination every other day with recording after recovery from surgery. After each discrimination session with recording, electrodes were advanced either 0.042 or 0.083 mm to record from new units the following session. For Experiment 2, there were 18 trials per session consisting of 6 danger trials, 5 uncertainty no-shock trials, 3 uncertainty shock trials, and 4 safety trials. Rats received an additional 3 sessions of fear discrimination during which the rats were connected to cables like those used during the optogenetic manipulation, but that did not deliver light, to habituate them to the cables. Thus, rats received a total of 19 fear discrimination sessions before the optogenetic manipulation. The order of trial type presentation was randomly determined by the behavioral program, and differed for each rat, each session for both experiments. Recording sessions contained more trials in order to maximize the number of units recorded per rat per session.

Single-unit data acquisition: During recording sessions, a 1x amplifying head stage connected the Omnetics connector to the commutator via a shielding recording cable. Analog neural activity was digitized and high-pass filtered via amplifier to remove low-frequency artifacts, and sent to the Ominplex D acquisition system (Plexon Inc., Dallas TX). Behavioral events (cues, shocks, nose pokes) were controlled and recorded by a computer running Med Associates software. Time-stamped events from Med Associates were sent to Ominplex D acquisition system via a dedicated interface module (DIG-716B). The result was a single file (.pl2) containing all time stamps for recording and behavior. Single-units were sorted offline with a template-based spike-sorting algorithm (Offline Sorter V3, Plexon Inc., Dallas TX). Time-stamped spikes and events (cues, shocks, nose pokes) were extracted (Neuroexplorer), and analyzed with statistical routines in MATLAB (Natick, MA).

Optogenetic manipulation: Rats underwent 3 sessions of vlPAG illumination via optical cables followed by 3 sessions without illumination or cables. The vlPAG was illuminated during the foot shock on uncertainty-shock and danger trials. Illumination on both uncertainty and danger trials occurred for 4 seconds, beginning immediately after auditory cue offset (2 s), continuing during foot shock (0.5 s), and ending 1.5 s after foot shock offset. Optical inhibition was achieved via delivery of 25 mW of 532 nm ‘green’ light on each side. Light was produced by a DPSS laser connected to an optical commutator attached to a custom made behavioral cable (Multimode Fiber, 0.22 NA, High-OH, Ø200 μm Core),

which connected to the implanted optical ferrule (2.5mm OD, 230 um Bore Multimode Ceramic Zirconia). Light output of 25 mW was chosen based on calculations the optical fibers will produce ~5 mW/mm^2 of light at distance of 1.2 mm from fiber tip.

Histology: Rats were deeply anesthetized using isoflurane and perfused with 0.9% biological saline and 4% paraformaldehyde in a 0.2 M Potassium Phosphate Buffered Solution. Final electrode coordinates were marked by passing a brief current from a 6V battery through 4 of the 16 Nichrome electrode wires. Brains were extracted and post-fixed in a 10% neutral-buffered formalin solution for 24 hrs, stored in 10% sucrose/formalin, frozen at −80°C and sectioned via a sliding microtome. Brains with electrodes were processed for light microscopy using anti-tryptophan hydroxylase immunohistochemistry. Sections were mounted on glass microscope slides, imaged using a light microscope, and electrode placement confirmed (Paxinos & Watson, 2007). Brains with optical implants were processed for fluorescent microscopy. Sections were mounted on glass microscope slides, coverslipped using VECTASHIELD HardSet Antifade Mounting Medium with DAPI (Vector Laboratories, Burlingame, CA), and viral transfection and optical implant sites were confirmed(Paxinos & Watson, 2007). A subset of tissue was processed with fluorescent anti-tryptophan hydroxylase immunohistochemistry and NeuroTrace™ in order to ensure viral transfections did not diffuse into the dorsal raphe nucleus. This tissue was mounted on glass slides with VECTASHIELD HardSet Antifade Mounting Medium.

QUANTIFICATION AND STATISTICAL ANALYSIS

Baseline nose poke analyses—For both experiments, the time stamp for every nose poke and event onset (cues and shocks) during each session was recorded automatically. Raw data were processed in MATLAB to extract nose poke rates during two periods: the baseline, which was 20 seconds prior to cue onset, and the 10-s cue. Baseline nose pokes are reported in pokes/min and analyzed with ANOVA.

Calculating and analyzing suppression ratios—For both experiments, suppression of rewarded nose poking was used as the behavioral indicator of fear. Nose poke rates were calculated for two temporal windows. A suppression ratio for total cued fear was calculated from nose poke rates during a 20 s baseline period just prior to cue onset and the 10 s cue period: (baseline - cue / baseline + cue). Complete nose poke suppression was signified by a suppression ratio of ‘1.00’ during the cue relative to baseline, indicating a high level of fear. No nose poke suppression was signified by a suppression ratio of ‘0.00,’ indicating no fear. Intermediate values indicated graded levels of fear.

Identifying shock-responsive neurons—All neurons were screened for excitatory firing during the 1500 ms period starting with the 500 ms shock period and continuing for next 1000 ms. This was achieved using a paired, two-tailed t-test comparing raw firing rate (spikes/s) during a 2 s baseline period just prior to shock onset and firing rate (spikes/s) during the 1500 ms interval. Two tests were performed for each neuron, one for danger and one for uncertainty-shock, and $p < 0.025$ was considered significant (Bonferroni correction for two tests).

Normalization of firing—For each neuron, and for each trial type, firing rate (spikes/s) was calculated in 100 ms bins from 20 s prior to cue onset to 20 s following cue offset. Differential firing was calculated for each bin by subtracting mean baseline firing rate (2 s prior to cue onset), specific to that trial type. Mean differential firing was Z-score normalized across all trial types within a single neuron, such that mean firing = 0, and standard deviation in firing = 1. Z-score normalization was applied to firing across the entirety of the recording epoch, as opposed to only the baseline period, in case neurons showed little/no baseline activity. Z-score normalized firing was analyzed with ANOVA using bin and trial-type as factors. F and p values are reported, as well as partial eta squared and observed power.

Population and single-unit firing analyses—Firing for the shock-responsive population was analyzed with ANOVA with trial type (danger, uncertainty-shock, uncertainty-omission, and safety) and 100 ms bins as factors. Bins spanned from cue offset to 3 s post-shock offset (5 s total = 50 bins). Paired t-tests and sign tests were used to compare firing in the 500 ms bin following shock offset. Pearson's correlation coefficient was then applied to determine the relationship between firing on danger and uncertainty-shock trial types.

Single-unit regression—Single-unit, linear regression was used to determine the degree to which predicted or surprising foot shock explained trial-by-trial variation in firing of single neurons in 500 ms intervals across the post-cue period. For each regression, all 32 trials from a single session were ordered by type. Z-firing was specified for the interval of interest. The 'predicted' regressor assigned the following values to each trial type: (danger = 2, unc-shock = 1, unc-omission = 0, safety = 0), while the 'surprising' regressor assigned: (danger = 1, unc-shock = 2, unc-omission = 0, safety = 0). Regression (using the regress function in Matlab) required a separate, constant input. Output was the beta coefficient for each regressor, quantifying the strength (greater distance from zero = stronger) and direction (>0 = positive) of the predictive relationship between each regressor and single-unit firing. ANOVA, two-tailed dependent samples t-test, sign test and Pearson's correlation coefficient were all used to analyze beta coefficients, exactly as described for normalized firing.

Session-by-session analyses for behavior—ANOVA for suppression ratios with between factors of group (eNpHR vs. YFP) and sex (female vs male), plus within factors of session (2 pre-exposure, 16 discrimination, and 3 tethered) and cue (danger vs. uncertainty vs. safety) were used compare pre-illumination behavior. An identical ANOVA but for 6 sessions during and following illumination (3 illumination and 3 tethered) were performed to determine the effects of optogenetic inhibition.

Trial-by-trial analyses for firing and behavior—For each shock-responsive unit, the first three uncertainty-shock trials were identified (trial n). Differential firing was calculated for each trial by taking Z firing to uncertainty shock in the 500 ms post shock period, minus mean Z firing of the six danger trials in the same post-shock period. Positive differential firing would indicate +PE (uncertainty-shock > danger) while ~zero or negative differential firing would indicate absence of +PE. For each 'n' trial the next three uncertainty trials were

identified, irrespective of shock contingency (n+1, n+2 and n+3). Suppression ratios for uncertainty were calculated for each trial (n, n+1, n+2 and n+3). Analysis of covariance (ANCOVA) was used to determine if differential firing on trial 'n' informed the pattern of suppression ratio to uncertainty over trials n, n+1, n+2 and n+3. Between subjects t-test on median split data and Pearson's correlation coefficient were further used to determine significance of the relationship between differential firing and change in suppression ratio.

For the second illumination session, the first uncertainty-shock and danger trials (n) were identified for each subject. For each uncertainty 'n' trial the next three uncertainty trials were identified, irrespective of shock contingency (n+1, n+2 and n+3) and the same was done for danger. Suppression ratios for uncertainty were calculated for each trial (n, n+1, n +2 and n+3). ANOVA with between subjects factors of group (YFP vs. eNpHR) and sex (female vs. male), plus within subjects factors of trial (n+1, n+2 and n+3) and cue (danger vs. uncertainty) was used to determine trial-by-trial changes in fear to each cue. Between subjects t-test for difference score was used to compare changes in YFP and eNpHR rats.

DATA AND SOFTWARE AVAILABILITY

The electrophysiology data set will be uploaded to http://crcns.org/ upon acceptance for publication. The optogenetics data will be uploaded to Harvard Dataverse repository.

ADDITIONAL RESOURCES

Med Associates programs used for behavior and MATLAB programs used for behavioral analyses are made freely available at our lab website: http://mcdannaldlab.org/resources

Supplementary Material

Refer to Web version on PubMed Central for supplementary material.

Acknowledgments:

This work was supported by grants from NIDA and NIMH (MAM). We thank Bret Judson and the Boston College Imaging Core for infrastructure and support.

Abbreviations:

lPAG	lateral periaqueductal grey
+PE	positive prediction error
TH+	tyrosine hydroxylase positive
vlPAG	ventrolateral periaqueductal grey
vGluT2	vesicular glutamate transporter 2
Unc-S	uncertainty-shock
Unc-O	uncertainty-omission

References

Assareh N, Bagley EE, Carrive P, & McNally GP (2017). Brief optogenetic inhibition of rat lateral or ventrolateral periaqueductal gray augments the acquisition of Pavlovian fear conditioning. Behav Neurosci, 131(6), 454–459. doi:10.1037/bne0000217 [PubMed: 29083203]

Assareh N, Sarrami M, Carrive P, & McNally GP (2016). The Organization of Defensive Behavior Elicited by Optogenetic Excitation of Rat Lateral or Ventrolateral Periaqueductal Gray. Behavioral Neuroscience, 130(4), 406–414. doi:10.1037/bne0000151 [PubMed: 27243807]

Beitz AJ (1982). The organization of afferent projections to the midbrain periaqueductal gray of the rat. Neuroscience, 7(1), 133–159. [PubMed: 7078723]

Berg BA, Schoenbaum G, & McDannald MA (2014). The dorsal raphe nucleus is integral to negative prediction errors in Pavlovian fear. European Journal of Neuroscience, 40(7), 3096–3101. [PubMed: 25041165]

Calu DJ, Roesch MR, Haney RZ, Holland PC, & Schoenbaum G (2010). Neural correlates of variations in event processing during learning in central nucleus of amygdala. Neuron, 68(5), 991–1001. [PubMed: 21145010]

Cho JR, Treweek JB, Robinson JE, Xiao C, Bremner LR, Greenbaum A, & Gradinaru V (2017). Dorsal Raphe Dopamine Neurons Modulate Arousal and Promote Wakefulness by Salient Stimuli. Neuron, 94(6), 1205–1219 e1208. doi:10.1016/j.neuron.2017.05.020 [PubMed: 28602690]

Cole S, & McNally GP (2009). Complementary roles for amygdala and periaqueductal gray in temporal-difference fear learning. Learn Mem, 16(1), 1–7. doi:10.1101/lm.1120509 [PubMed: 19117910]

Dannlowski U, Stuhrmann A, Beutelmann V, Zwanzger P, Lenzen T, Grotegerd D, … Kugel H (2012). Limbic scars: long-term consequences of childhood maltreatment revealed by functional and structural magnetic resonance imaging. Biol Psychiatry, 71(4), 286–293. doi:10.1016/j.biopsych.2011.10.021 [PubMed: 22112927]

DiLeo A, Wright KM, & McDannald MA (2016). Sub-second fear discrimination in rats: Adult impairment in adolescent heavy alcohol drinkers. Learning & Memory, 23, 618–622. [PubMed: 27918281]

Floyd NS, Price JL, Ferry AT, Keay KA, & Bandler R (2000). Orbitomedial prefrontal cortical projections to distinct longitudinal columns of the periaqueductal gray in the rat. J Comp Neurol, 422(4), 556–578. [PubMed: 10861526]

Grahn RE, Will MJ, Hammack SE, Maswood S, McQueen MB, Watkins LR, & Maier SF (1999). Activation of serotonin-immunoreactive cells in the dorsal raphe nucleus in rats exposed to an uncontrollable stressor. Brain Res, 826(1), 35–43. [PubMed: 10216194]

Groessl F, Munsch T, Meis S, Griessner J, Kaczanowska J, Pliota P, … Haubensak W (2018). Dorsal tegmental dopamine neurons gate associative learning of fear. Nat Neurosci, 21(7), 952–962. doi:10.1038/s41593-018-0174-5 [PubMed: 29950668]

Grupe DW, & Nitschke JB (2013). Uncertainty and anticipation in anxiety: an integrated neurobiological and psychological perspective. Nat Rev Neurosci, 14(7), 488–501. doi:10.1038/nrn3524 [PubMed: 23783199]

Johansen JP, Tarpley JW, LeDoux JE, & Blair HT (2010). Neural substrates for expectation-modulated fear learning in the amygdala and periaqueductal gray. Nat Neurosci, 13(8), 979–986. doi:10.1038/nn.2594 [PubMed: 20601946]

Li C, Sugam JA, Lowery-Gionta EG, McElligott ZA, McCall NM, Lopez AJ, … Kash TL (2016). Mu Opioid Receptor Modulation of Dopamine Neurons in the Periaqueductal Gray/Dorsal Raphe: A Role in Regulation of Pain. Neuropsychopharmacology, 41(8), 2122–2132. doi:10.1038/npp.2016.12 [PubMed: 26792442]

Matthews GA, Nieh EH, Vander Weele CM, Halbert SA, Pradhan RV, Yosafat AS, … Tye KM (2016). Dorsal Raphe Dopamine Neurons Represent the Experience of Social Isolation. Cell, 164(4), 617–631. doi:10.1016/j.cell.2015.12.040 [PubMed: 26871628]

McNally GP, & Cole S (2006). Opioid receptors in the midbrain periaqueductal gray regulate prediction errors during pavlovian fear conditioning. Behav Neurosci, 120(2), 313–323. doi:10.1037/0735-7044.120.2.313 [PubMed: 16719696]

McNally GP, Johansen JP, & Blair HT (2011). Placing prediction into the fear circuit. Trends Neurosci, 34(6), 283–292. doi:10.1016/j.tins.2011.03.005 [PubMed: 21549434]

Ozawa T, Ycu EA, Kumar A, Yeh LF, Ahmed T, Koivumaa J, & Johansen JP (2017). A feedback neural circuit for calibrating aversive memory strength. Nature Neuroscience, 20(1), 90–97. doi:10.1038/nn.4439 [PubMed: 27842071]

Paxinos G, & Watson C (2007). The rat brain in stereotaxic coordinates (6th ed.). Amsterdam; Boston;: Academic Press/Elsevier.

Ray MH, Hanlon E, & McDannald MA (2018). Lateral orbitofrontal cortex partitions mechanisms for fear regulation and alcohol consumption. PLoS One, 13(6), e0198043. doi:10.1371/journal.pone.0198043 [PubMed: 29856796]

Rescorla RA (1970). Reduction in the effectiveness of reinforcement after prior excitatory conditioning. *Learning &* Motivation, 1, 372–381.

Rescorla RA, & Wagner AR (1972). A theory of Pavlovian conditioning: Variations in the effectiveness of reinforcement and nonreinforcement In AH B & WF P (Eds.), Classical Conditioning II: Current Research and Theory (pp. 64–99). New York: Appleton Century Crofts.

Roesch MR, Calu DJ, Esber GR, & Schoenbaum G (2010). Neural correlates of variations in event processing during learning in basolateral amygdala. Journal of Neuroscience, 30(7), 2464–2471. [PubMed: 20164330]

Roesch MR, Calu DJ, & Schoenbaum G (2007). Dopamine neurons encode the better option in rats deciding between differently delayed or sized rewards. Nature Neuroscience, 10(12), 1615–1624. [PubMed: 18026098]

Roy M, Shohamy D, Daw N, Jepma M, Wimmer GE, & Wager TD (2014). Representation of aversive prediction errors in the human periaqueductal gray. Nat Neurosci, 17(11), 1607–1612. doi:10.1038/nn.3832 [PubMed: 25282614]

Rozeske RR, Jercog D, Karalis N, Chaudun F, Khoder S, Girard D, … Herry C (2018). Prefrontal-Periaqueductal Gray-Projecting Neurons Mediate Context Fear Discrimination. Neuron, 97(4), 898–910 e896. doi:10.1016/j.neuron.2017.12.044 [PubMed: 29398355]

Sarlitto MC, Foilb AR, & Christianson JP (2018). Inactivation of the Ventrolateral Orbitofrontal Cortex Impairs Flexible Use of Safety Signals. Neuroscience, 379, 350–358. doi:10.1016/j.neuroscience.2018.03.037 [PubMed: 29604383]

Schultz W, Dayan P, & Montague PR (1997). A neural substrate of prediction and reward. Science, 275(5306), 1593–1599. [PubMed: 9054347]

Schweimer JV, & Ungless MA (2010). Phasic Responses in Dorsal Raphe Serotonin Neurons to Noxious Stimuli. Neuroscience, 171(4), 1209–1215. doi:10.1016/j.neuroscience.2010.09.058 [PubMed: 20888395]

Sengupta A, & McNally GP (2014). A role for midline and intralaminar thalamus in the associative blocking of Pavlovian fear conditioning. Front Behav Neurosci, 8, 148. doi:10.3389/fnbeh.2014.00148 [PubMed: 24822042]

Todd AJ (2010). Neuronal circuitry for pain processing in the dorsal horn. Nat Rev Neurosci, 11(12), 823–836. doi:10.1038/nrn2947 [PubMed: 21068766]

Vidal-Gonzalez I, Vidal-Gonzalez B, Rauch SL, & Quirk GJ (2006). Microstimulation reveals opposing influences of prelimbic and infralimbic cortex on the expression of conditioned fear. Learn Mem, 13(6), 728–733. doi:10.1101/lm.306106 [PubMed: 17142302]

Walker RA, Andreansky C, Ray MH, & McDannald MA (2018). Early Adolescent Adversity Inflates Threat Estimation in Females and Promotes Alcohol Use Initiation in Both Sexes. Behavioral Neuroscience, 132(3), 171–182. doi:10.1037/bne0000239 [PubMed: 29809045]

Watabe-Uchida M, Zhu L, Ogawa SK, Vamanrao A, & Uchida N (2012). Whole-brain mapping of direct inputs to midbrain dopamine neurons. Neuron, 74(5), 858–873. doi:10.1016/j.neuron.2012.03.017 [PubMed: 22681690]

Wright KM, DiLeo A, & McDannald MA (2015). Early adversity disrupts the adult use of aversive prediction errors to reduce fear in uncertainty. Front Behav Neurosci, 9, 227. doi:10.3389/fnbeh.2015.00227 [PubMed: 26379520]

Yau JO, & McNally GP (2015). Pharmacogenetic excitation of dorsomedial prefrontal cortex restores fear prediction error. J Neurosci, 35(1), 74–83. doi:10.1523/JNEUROSCI.3777-14.2015 [PubMed: 25568104]

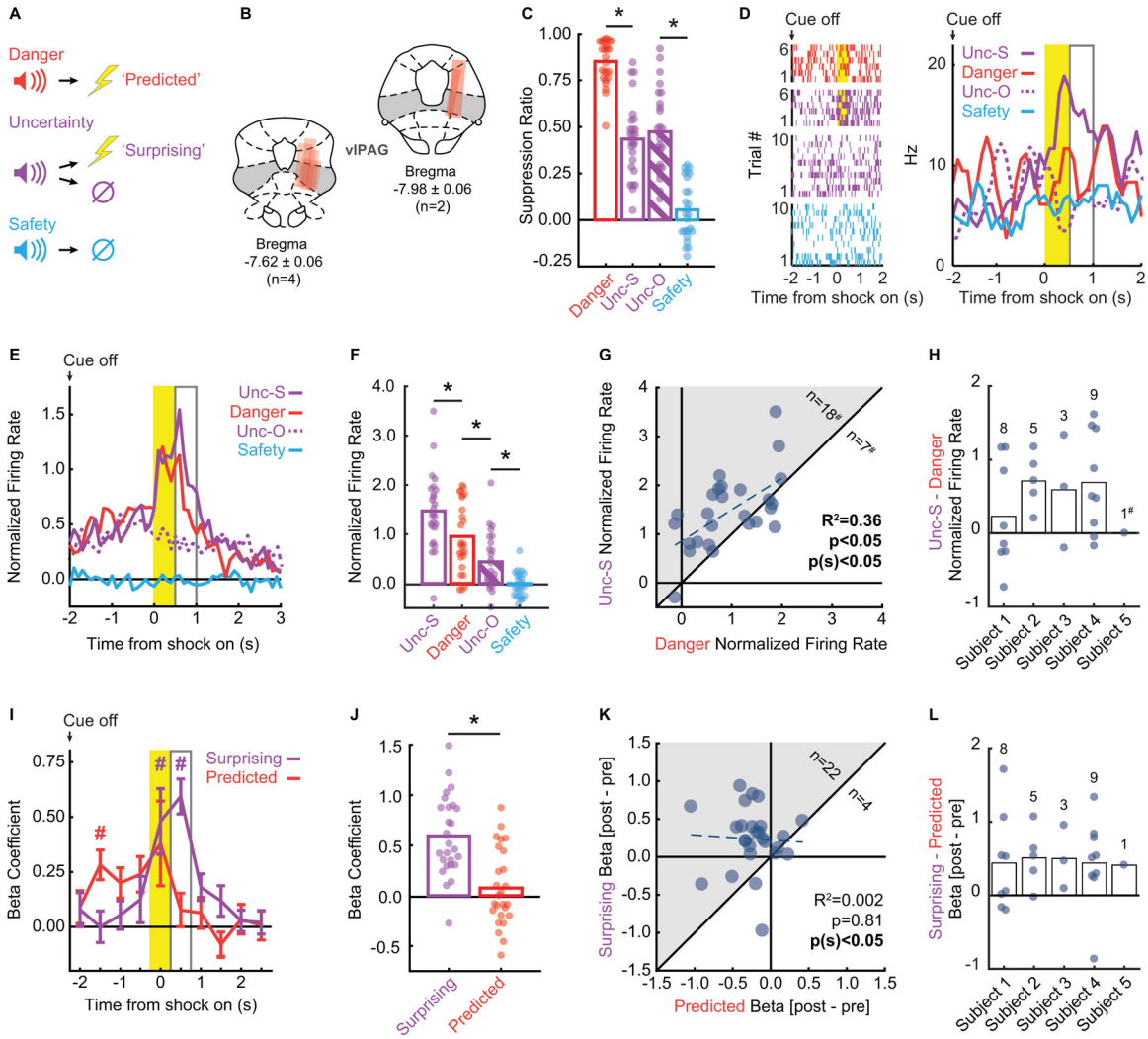

Figure 1. VlPAG single-unit activity signals +PE

A Pavlovian fear discrimination procedure: three auditory cues were associated with a unique probability of foot shock: danger, p = 1.00 (red); uncertainty, p = 0.375 (purple); and safety, p = 0.00 (blue). Suppression of rewarded nose poking was used as an indicator of fear.

B Microelectrode bundle placements for all rats (n = 6) and all neurons (n = 245) during recording sessions are represented by red bars. The majority of units were recorded from the ventrolateral subregion of the PAG (vlPAG).

C Mean suppression ratios for danger (red), uncertainty-shock (purple; Unc-S), uncertainty-omission (purple striped; Unc-O), and safety (blue) are shown for the 26 sessions in which shock-responsive neurons were recorded. Circles show suppression ratios from each individual session. Asterisks indicate significance of a between subject's t-test ($p < 0.05$).

D Raster plots (left) from a representative shock-responsive neuron during 4-s post-cue period is shown for the 6 danger trials (red, top), 6 uncertainty-shock trials (purple, 2nd from top), 10 uncertainty-omission trials (purple, 2nd from bottom), and 10 safety trials (bottom). Each tick represents an action potential. Mean firing rate (Hz, right) to danger (red),

uncertainty-shock (solid purple; Unc-S), uncertainty-omission (purple dashed; Unc-O), and safety (blue) trials are shown for the same unit. Yellow bar indicates 500-ms shock period, open gray bar the 500-ms post shock period.

E Mean normalized firing of the 26 shock-responsive neurons during the 5-s post-cue period is shown for danger (red), uncertainty-shock (solid purple; Unc-S), uncertainty-omission (purple dashed; Unc-O), and safety (blue) trials for shock-responsive neurons. Yellow bar indicates 500-ms shock period, open gray bar the 500-ms post shock period.

F Mean normalized firing rate to uncertainty-shock (purple; Unc-S), danger (red), uncertainty-omission (purple striped; Unc-O), and safety (blue) during the 500-ms following shock offset revealed significantly higher firing rates on uncertainty-shock compared to danger and the other trial types. Circles show normalized firing rates from each individual session. Asterisks indicate significance of a between subject's t-test ($p < 0.05$).

G Scatter comparing normalized firing on danger and uncertainty-shock trials in the 500-ms post shock period. Pearson's correlation coefficient, associated significance (p) and sign test significance [p(s)] are shown. Eighteen neurons showed greater firing on uncertainty trials compared to danger (gray region), seven showed greater firing on uncertainty trials and $^{\#}$one neuron showed equivalent firing.

H Differential firing in the 500-ms post-shock period (uncertainty shock – danger) is plotted for each subject (bar) and shock-responsive neuron (circle). $^{\#}$neuron showed no differential firing (0).

I Mean ± SEM beta coefficient for predicted (red) and surprising (purple) shock shown for each 500-ms interval. # indicates significance of single sample t-test compared to zero (Bonferroni correction, $p < 0.005$).

J Mean beta coefficient for surprising (purple) and predicted (red) shock shown for the 500-ms post shock period. Circles show beta coefficients for individual sessions. Asterisk indicates significance of a between subject's t-test ($p < 0.05$).

K Plotting differential pre- (mean of 3 pre-shock intervals) and post-shock (mean of 3 post-shock intervals) beta coefficients for predicted and surprising shock revealed a bias toward surprising shock (grey shaded area) in 22 of 26 units. Betas were significantly correlated as indicated by Pearson's R^2 ($p < 0.05$).

L Differential beta coefficient (post – pre) for predicted vs surprising regressor is plotted for each subject (bar) and shock-responsive neuron (circle).

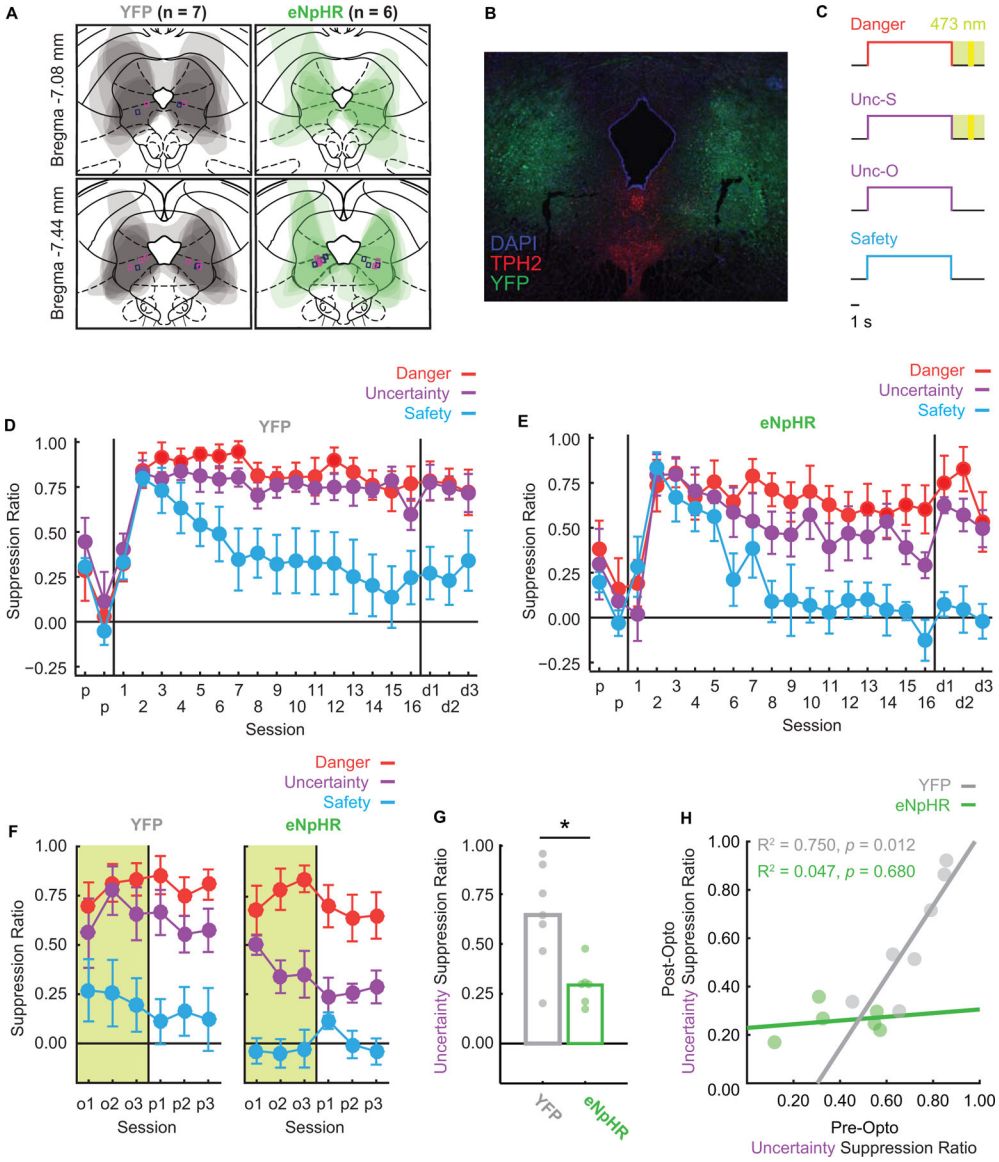

Figure 2. VlPAG optogenetic inhibition during foot shock decreases fear to uncertainty

A Viral transfection extent was mapped for all YFP (grey) and eNpHR (green) rats, and average transfection extent can be seen in their overlaid tracings. Rectangular markers indicate fiber optic ferrule placements (magenta = females; navy = males) were all within or on the border of vlPAG bounds.

B Representative viral transfection is shown with YFP (green), TPH2 (red), and DAPI (blue). Fiber optic ferrule placement can be seen in the vlPAG in both the left and right hemispheres. Note ferrule placement shows exaggerated damage due to immunohistochemistry processing.

C During optogenetic sessions, green-light illumination began at cue offset, continued during the 0.5-s shock (yellow period), and lasted 1.5 s after shock for a total of 4 s. Note illumination never occurred during cue periods.

D Mean ± SEM suppression ratios for YFP rats to danger (red), uncertainty (purple), and safety (blue) are shown for the 2 pre-exposure sessions (p), 16 discrimination sessions (1–16), and 3 dummy cable discrimination sessions (d1–d3).
E eNpHR suppression ratio data shown as in C.
F Mean ± SEM suppression ratios for YFP rats (left) and eNpHR rats (right) to danger (red), uncertainty (purple), and safety (blue) over the 3 sessions of optogenetic manipulation (o1–o3) and 3 post-manipulation sessions (p1–p3).
G Mean suppression ratios to uncertainty during the last two sessions of optogenetic manipulation and the three post-manipulation sessions (5 sessions total) is shown for YFP (gray bar) and eNpHR rats (green bar). Circles show average suppression ratios for individual rats. Asterisk indicates significance of a between subject's t-test ($p < 0.05$).
H Mean uncertainty suppression ratio for the final three discrimination sessions (pre-opto) is plotted against mean uncertainty suppression ratio for the three sessions following illumination (post-opto). Data shown for each YFP (gray) and eNpHR individual (green) along with R^2 and p-value.

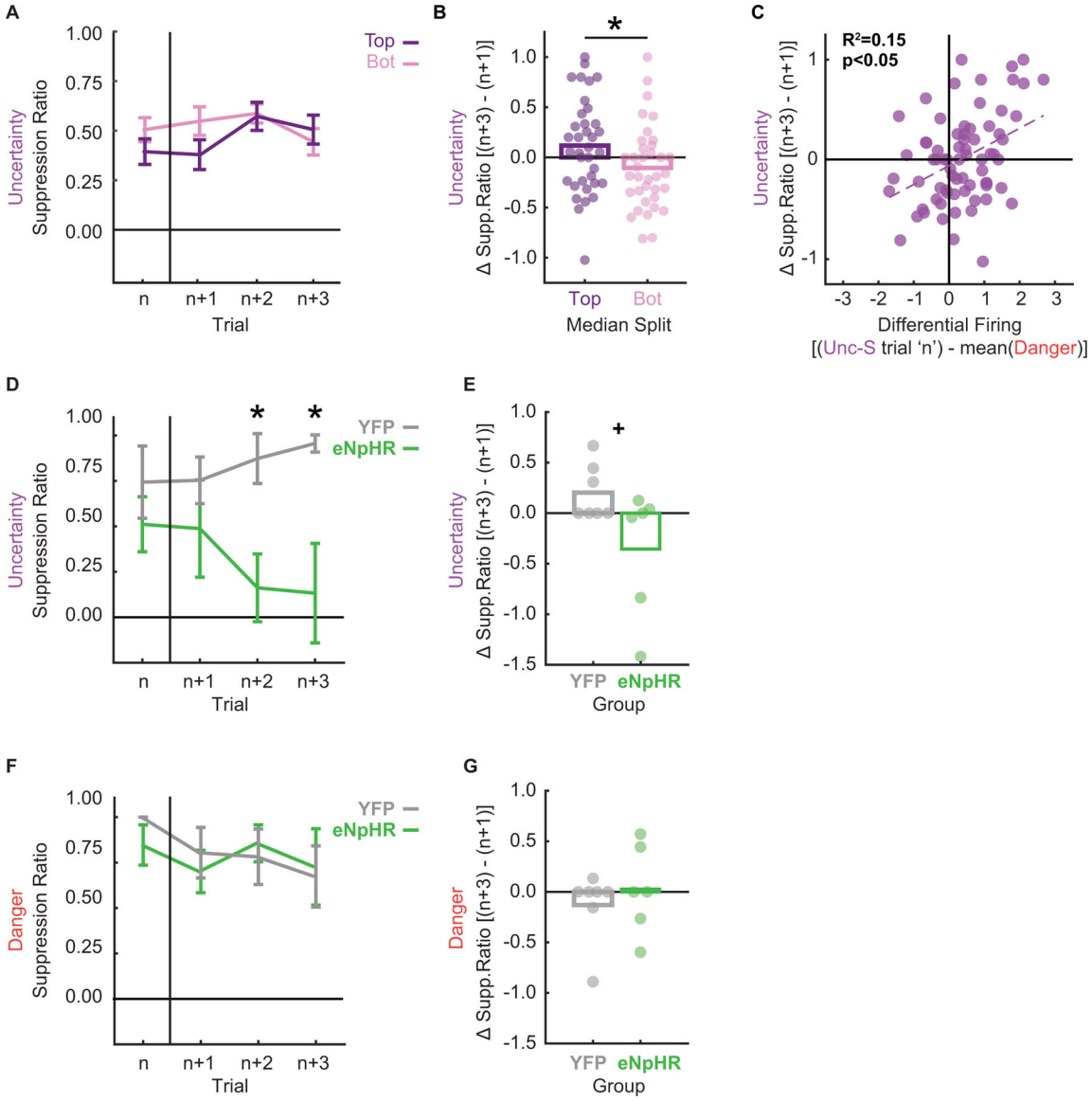

Figure 3. VlPAG +PE updates within session fear behavior

A Mean ± SEM suppression ratio is shown for uncertainty-shock trials (n) and the next three uncertainty trials irrespective of shock or omission (n+1, n+2 and n+3). The 71 total sequences were split according to +PE firing on trial 'n', top 35 shown in purple, bottom 36 shown in pink.

B + or – Mean change in suppression ratio [(n+3) – (n+1)] is shown for the top 35 (purple) and bottom 36 (pink) sequences. Data as in A. Circles show differences for individual sequences. Asterisk indicates significance of a between subject's t-test ($p < 0.05$).

C Differential firing [(Unc-S trial 'n') - mean(Danger)] was plotted against change in suppression ratio to uncertainty. Data points represent each trial n identified as in A and B. Pearson's R^2 and associated significance ($p < 0.05$) shown.

D Mean ± SEM suppression ratio is shown for the first uncertainty-shock trial (n) and the next three uncertainty trials irrespective of shock or omission (n+1, n+2 and n+3) for

illumination session 2 (YFP, gray and eNpHR, green). Asterisks indicate significance of between subject's t-test ($p < 0.05$).

E + or – Mean change in suppression ratio [(n+3) – (n+1)] is shown for YFP (gray) and eNpHR (green) rats. Data as in D. Circles show differences for individual rats. + indicates trend toward significance from a between subject's t-test ($p = 0.056$).

F Suppression ratios to the danger cue were plotted for trial n (here the first danger trial on optogenetic session 2) and the subsequent 3 danger trials in order to assess trial-by-trial changes in fear. YFP (grey line) and eNpHR (green line) rats showed equivalent levels of fear and no significant changes in fear to danger across trials.

G Average change in fear to the danger cue three trials after trial n compared to the first trial after n is graphed for YFP (grey bar) and eNpHR (green bar) rats. Circles show differences for individual rats. No significant change in fear to the danger cue occurred for either group.

KEY RESOURCES TABLE

REAGENT or RESOURCE	SOURCE	IDENTIFIER
Antibodies		
VECTASTAIN Elite ABC HRP Kit (Peroxidase, Sheep IgG)	Vector Laboratories	Cat# PK-6106
VECTOR NovaRED Peroxidase (HRP) Substrate Kit	Vector Laboratories	Cat# SK-4800
VECTASHIELD HardSet Antifade Mounting Medium with DAPI	Vector Laboratories	Cat# H-1500
VECTASHIELD HardSet Antifade Mounting Medium	Vector Laboratories	Cat# H-1400
NeuroTrace™ 435/455 Blue Fluorescent Nissl Stain	Thermo Fisher Scientific	Cat# N21479
Sheep Anti-Tryptophan Hydroxylase	Sigma	Cat# T8575
Alexa Fluor® 594 AffiniPure Donkey Anti-Sheep IgG (H+L)	Jackson Immuno	Cat# 713-585-147
Viruses		
AAV-hSyn-eNpHR3.0-EYFP (Stereotype 5)	UNC Vector Core	N/A
AAV-hSyn-EYFP (Stereotype 5)	UNC Vector Core	N/A
Deposited Data		
To be submitted on acceptance	This work	
Software and Algorithms		
MED PC-IV	Med Associates	
OmniPlex	Plexon	
Offline Sorter V6	Plexon	
NeuroExplorer	Plexon	
MATLAB	Mathworks	
SPSS	IBM	
Adobe Illustrator	Adobe	
Adobe Photoshop	Adobe	